SESSION 1

Chairman: W. G. Elford

https://doi.org/10.1017/S0074180900019586 Published online by Cambridge University Press

1. THE RADAR METEOR ECHO

(Survey Paper)

P. M. MILLMAN
(National Research Council, Ottawa, Canada)

From about 1930 on various scattered notes appeared from time to time, pointing out certain radio effects that probably resulted from meteors. However, the real birth of the serious observation of meteors by radio took place on the night of October 9–10, 1946, when the Giacobinid meteor shower returned in considerable strength. This was observed with re-built World-War II radar equipment in both England and the U.S.A., and the results achieved left no doubt concerning the value of the new technique in meteoric astronomy. Figure 1 illustrates two historic examples of meteor echoes recorded in England on this occasion (Appleton and Naismith, 1947; Hey *et al.*, 1947). Since this date the field has expanded rapidly. Useful general summaries may be found in a number of monographs, e.g., Lovell (1954), McKinley (1961).

The great majority of radio-meteor programs have employed the pulsed technique of radar, and the echoes are normally displayed with time as the abscissa, and some other property of the echo, such as range or amplitude, as ordinate. The examples in Figure 1 are both range-time plots using the pulsed technique. Useful information can also be obtained by using a continuous wave (CW) technique. Figure 2 illustrates examples of Geminid meteor echoes, secured with the CW equipment at Ottawa on December 13, 1950. This method of observation provides a continuous measure of the echo phase, but does not supply absolute range.

The meteor echo originates in a column of free electrons left by the meteor along its trajectory, and most meteor echoes are observed in the height range 70–120 km. The principal parameters of the meteor echo that can be measured directly are *range* (distance from the observer), *amplitude* (received power), and *phase*. Since these are normally recorded against a standard time system, this gives a fourth parameter, *duration* (length of time echo is observed). On the physical side meteor echoes divide themselves naturally into two categories, underdense and overdense.

In the case of the underdense echo the density of electrons is not great enough to prevent the incident radio wave from being scattered by each electron individually. The echo is highly aspect sensitive, maximum intensity resulting when the incident and scattered wave are perpendicular to the length of the column, or meteor trajectory. The point where the perpendicular from the radar equipment meets the meteor trajectory is frequently designated the T_0 point, and the typical Fresnel-zone patterns

Kresák and Millman (eds.), Physics and Dynamics of Meteors, 3–13. © *I.A.U.*

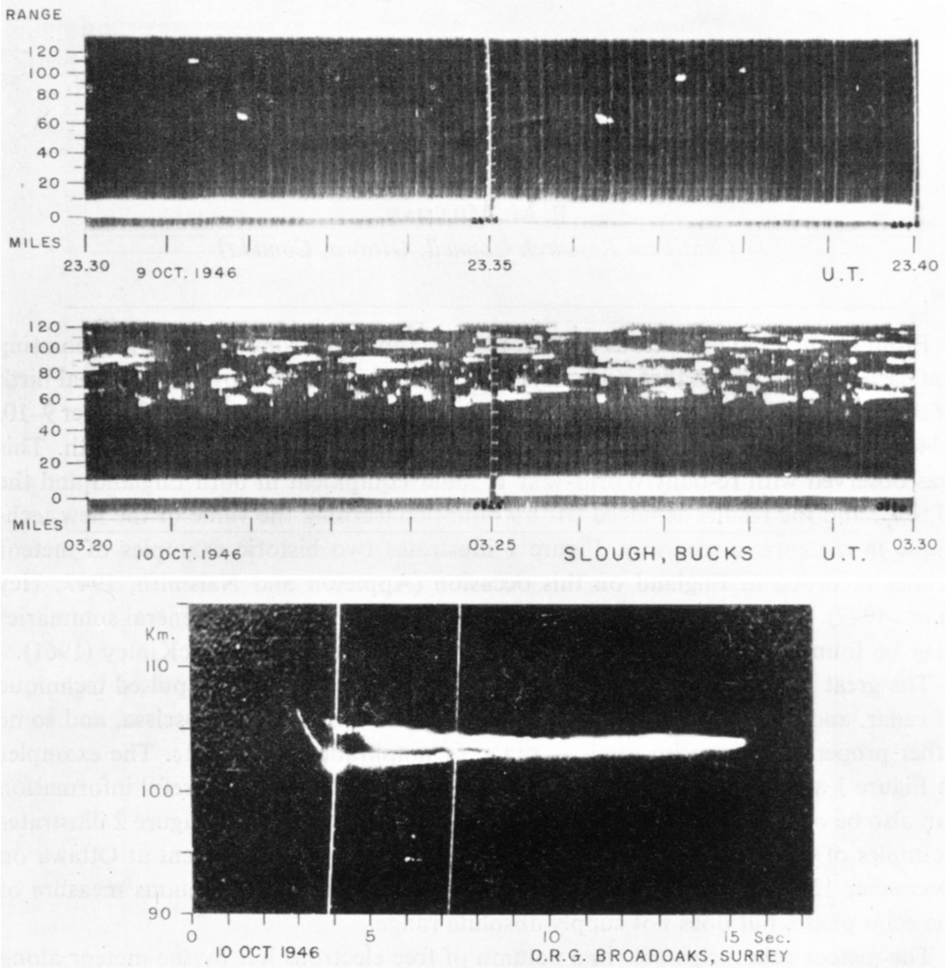

FIG. 1. *(above) Examples of two range-time radar records made on the night of the maximum of the Giacobinid meteor shower in 1946, with equipment operating at a frequency of 27 MHz. (Courtesy of E. Appleton and R. Naismith.) – (below) The echo of a Giacobinid meteor, showing a well-developed head echo from which the velocity of the meteor can be calculated. (Courtesy of J.S. Hey, S.J. Parsons, and G.S. Stewart.)*

about this point are seen in the meteor echoes of Figure 2. It can be shown theoretically that in general the amplitude of the underdense echo will rise sharply and decay exponentially with time, and this has been verified observatio.

If the meteor is large enough to leave an electron column with a volume density greater than the critical density, i.e. where the effective dielectric constant is zero or less for the wavelength used, then we have an overdense echo. In this case the elec-

https://doi.org/10.1017/S0074180900019586 Published online by Cambridge University Press

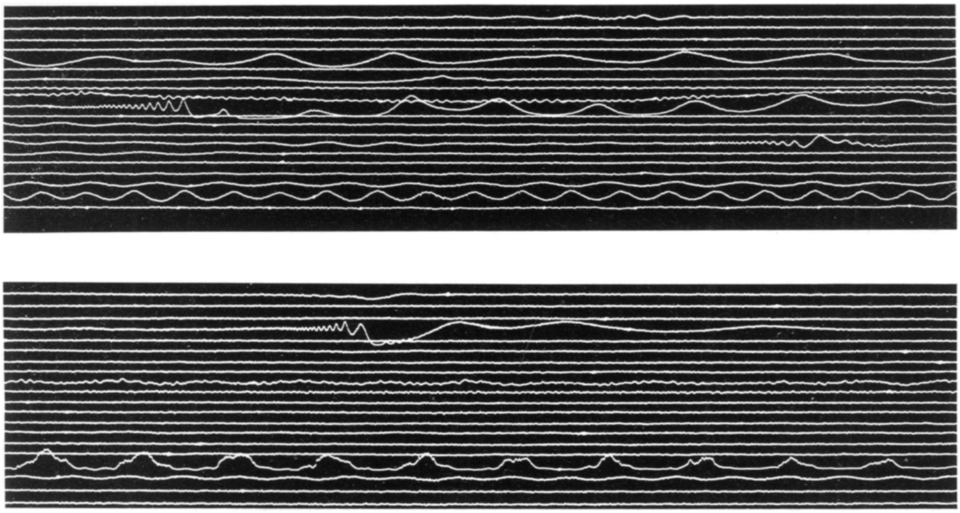

FIG. 2. *Examples of the fast doppler (CW) records made at Ottawa on December 13, 1950, near the peak of the Geminid shower. Seconds' markers and 1/10 sec markers appear as bright dots on the trace of echo amplitude. Time runs alternatively left and right on successive traces. The horizontal width reproduced represents just over one second on the time-scale.*

trons do not scatter individually and the incident wave does not fully penetrate the column. The line density of electrons, q, which marks the transition between underdense and overdense trails is somewhere near 10^{14} electrons/meter for average observational conditions. This line density corresponds roughly to the visual limit for faint meteors at magnitude $+5$. Hence most meteors seen visually produce overdense types of echoes, but individual cases may vary widely from the statistical norm.

The received power of the underdense echo varies as q^2, while the received power of the overdense echo varies as $q^{1/2}$. In the latter case the amplitude may rise gradually as the column expands and is distorted, and it may be some seconds before it will return an echo on the relevant wavelength. Further distortions by upper-air winds may produce several independent echo sources and mutual interference can result in rapid fading that is often periodic or semi-periodic. In the upper part of the meteor-echo height range the duration of the overdense echo varies directly as q and as the square of the wavelength, and inversely as the diffusion coefficient. As we go to lower levels the diffusion becomes less important and the mechanism of electron attachment becomes dominant, producing an effective upper limit to echo durations under normal ionospheric conditions.

Figure 3, taken from an earlier paper (Millman, 1962), illustrates the basic geometry of the formation of overdense meteor echoes in a range-time radar presentation. The important fact to bear in mind is that a meteor moving past an observer at constant velocity on a straight-line trajectory traces out an hyperbola on the range-

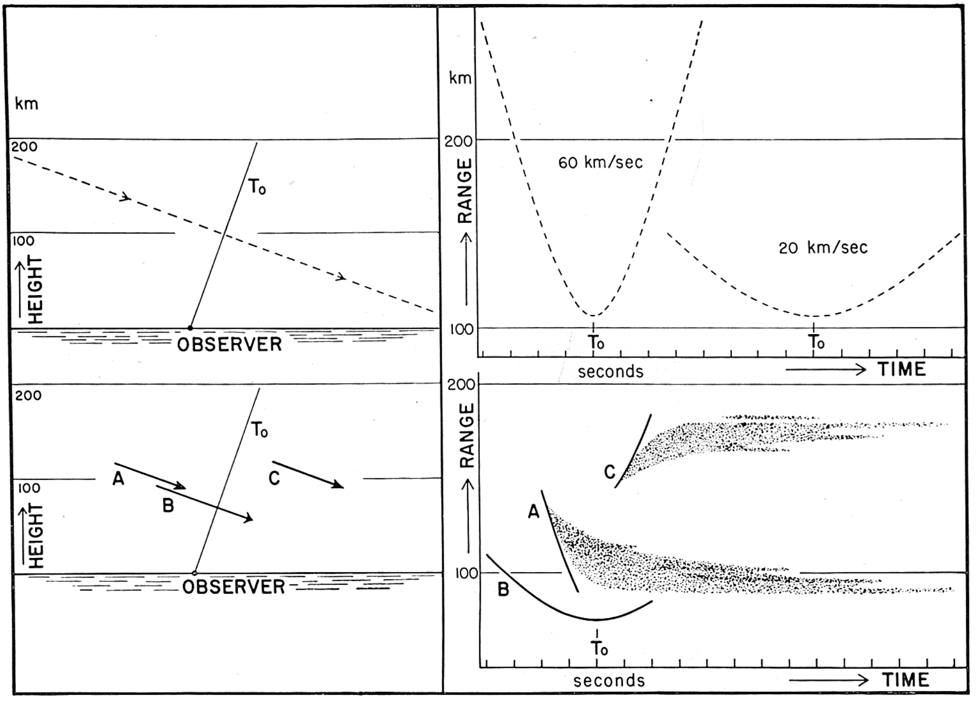

FIG. 3. *The geometry of the range-time presentation of radar meteor echoes. Left: meteor trajectories seen in vertical elevation. Right: the projection of the trajectories on a range-time plot, illustrating head echoes and typical overdense enduring echoes.*

time presentation. While echoes from underdense trails are normally only detected from the neighbourhood of the T_0 point, overdense trails may return an echo at all angles to their length, and thus stand a much greater chance of being recorded. This observational selection effect, which favours the overdense trails and therefore the brighter meteors, is an important factor to remember when dealing with the statistics of radar meteor counts.

In this brief introductory survey it is not possible even to list, much less to discuss in detail, the many problems involved in the interpretation of the radio observations of meteors. However, to provide a background for the papers to follow, I would like to present a picture gallery (Figures 4–11) of typical meteor echoes, taken from the records of the high-power meteor radar at the Springhill Observatory (lat. 45·2°N, long. 75·5°W) for the period from August 1966 to May 1967. This high-power equipment operates on 32 MHz with simple dipole transmitting and receiving antennas, and peak power in the 3–4 megawatt range. Pulse length is 12 μsec and pulse recurrence frequency about 117/sec. All records reproduced consist of a range-time presentation below and an amplitude-time presentation above. Seconds' markers appear near top and bottom of the range-time record, and range markers appear every 20 km as dark horizontal lines, except for the 100, 200, and 300 km markers, which are bright. The amplitude scale is logarithmic and only echoes in the range interval 60–260 km are recorded here. Most of the echoes reproduced were recorded while a visual team of eight observers and a recorder were active at Springhill. Where known, the shower association of a meteor echo is given by P = Perseid, L = Leonid, G = Geminid, N = non-shower, followed by the visual magnitude if the meteor was visually recorded. Time of the beginning of the echo is given by year, month, day, hour, minute, and second of Universal Time. To convert to local mean time subtract $5^h1^m53^s$. The echo classification is on the system established in Ottawa in 1947–48 (McKinley and Millman, 1949).

Figures 4 and 5 illustrate a number of echoes that are returned from a single range only (F type). Those of shortest duration are underdense, and the exponential decay is clearly evident as a straight line on the logarithmic amplitude plot. Examples are included grading all the way from echoes at the transition between underdense and overdense up to long duration echoes with various types of fading frequency. In some cases only an illustrative portion of an echo is reproduced.

Figure 6 shows a somewhat more complicated enduring echo with evidence of the echo source at more than one discrete range and a very regular type of fading with a period near half a second. At the beginning of this echo is a narrow line, a head echo (*h* characteristic), which is of very short duration at any given range, and generally follows the geometric trace of the meteor along its trajectory. Figure 7 illustrates a number of head echoes of approaching meteors, the second cut being a portion of the record of the strong Leonid return in 1966 where thousands of head echoes were evident. Additional head echoes as well as a multiplicity of echo ranges are shown in Figure 8. Note particularly the complicated nature of the echo as seen in the amplitude plot. It is obvious that a considerable number of individual components combine to give the total effect.

Figure 9 gives examples of two head echoes that have a range spread of over 100 km. These are typical of cases of bright meteors with a radiant at low elevation so that the meteor is moving nearly horizontally and remains in the meteor-echo height zone for several seconds. The Perseid meteor here has a long duration, with a very detailed echo of low amplitude. A somewhat more diffuse echo follows immediately after the central portion of the true head echo. This has been observed in a number of cases (Millman, 1962, Figure 4, Echo J) and gives warning that one must take care not to classify every sloping echo line as a head echo (McIntosh, 1962). Another point, illustrated by this Perseid echo, is that the lower edge of the filled in echo (*b* characteristic) may simulate the minimum-range portion of the hyperbolic trace, while the true minimum range for the given meteor trajectory is much lower. This effect results from the successively longer delays in the appearance of the *b* characteristic as we go to lower levels in the atmosphere. Here it takes longer for

https://doi.org/10.1017/S0074180900019586 Published online by Cambridge University Press

Typical examples of meteor radar echoes recorded at the Springhill Meteor Observatory, National Research Council, Ottawa.

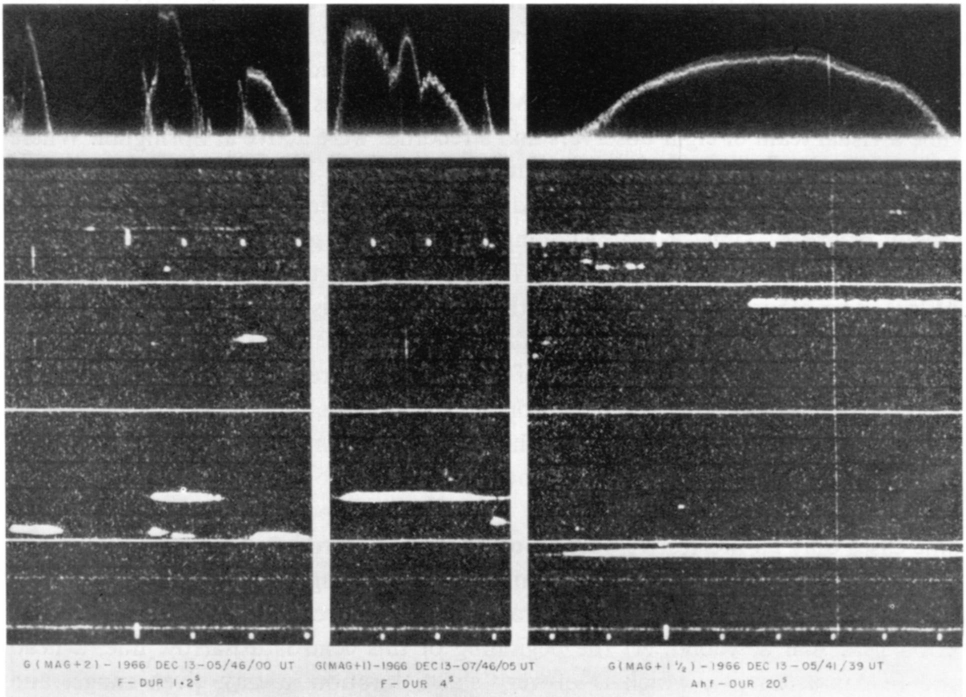

FIG. 4.

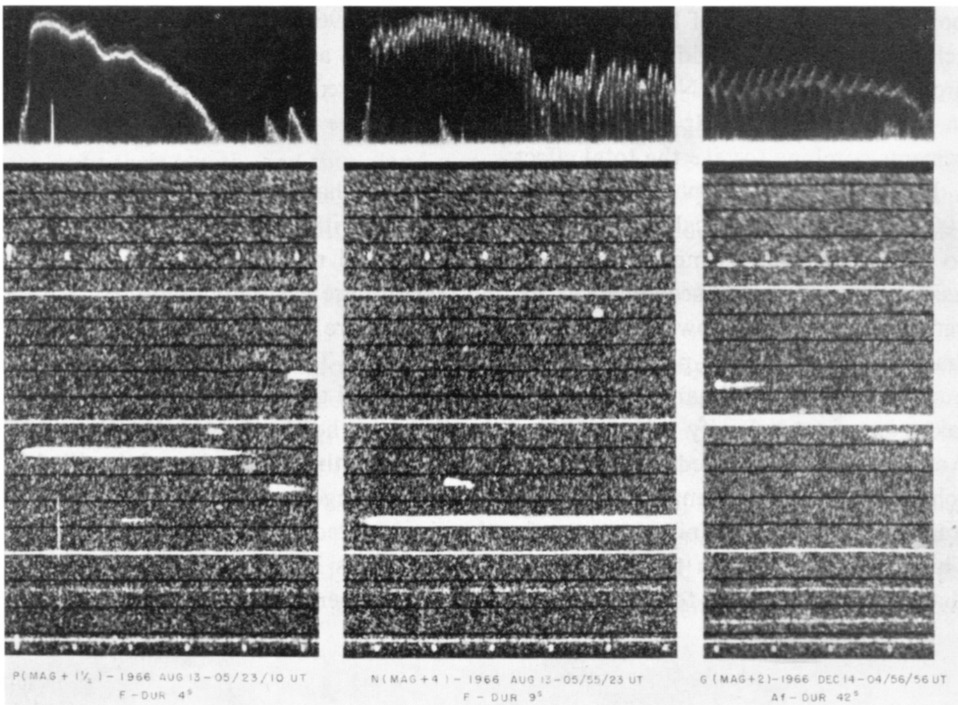

FIG. 5.

https://doi.org/10.1017/S0074180900019586 Published online by Cambridge University Press

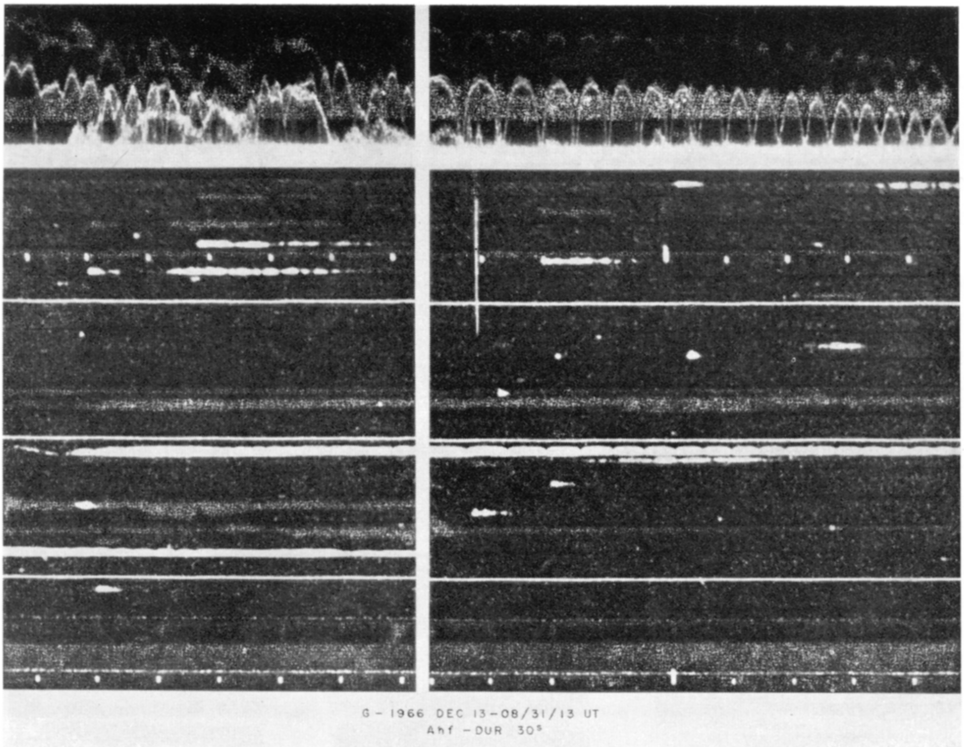

FIG. 6.

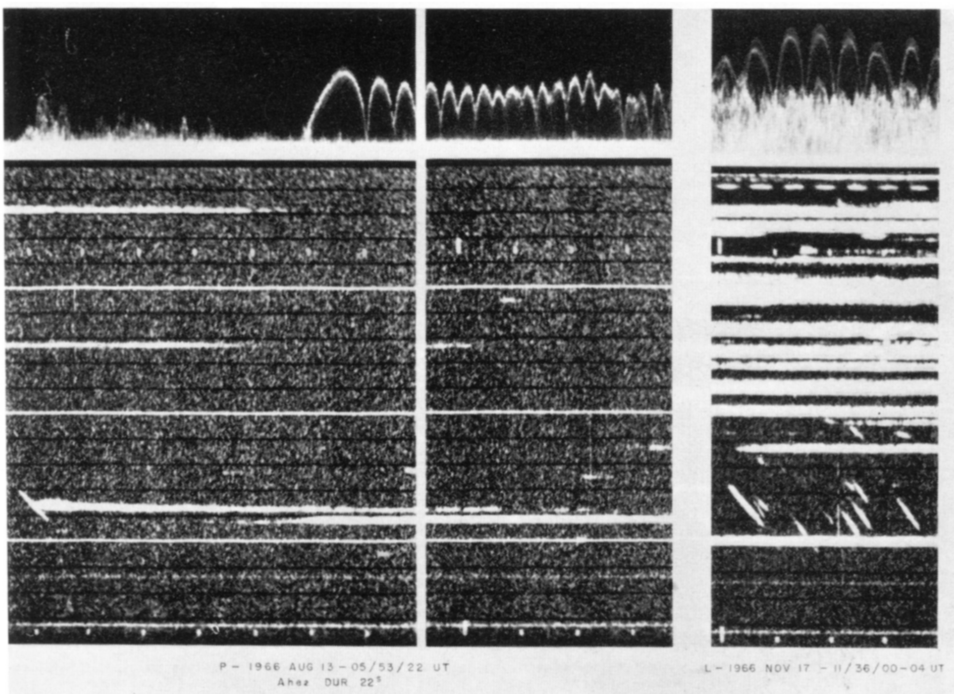

FIG. 7.

https://doi.org/10.1017/S0074180900019586 Published online by Cambridge University Press

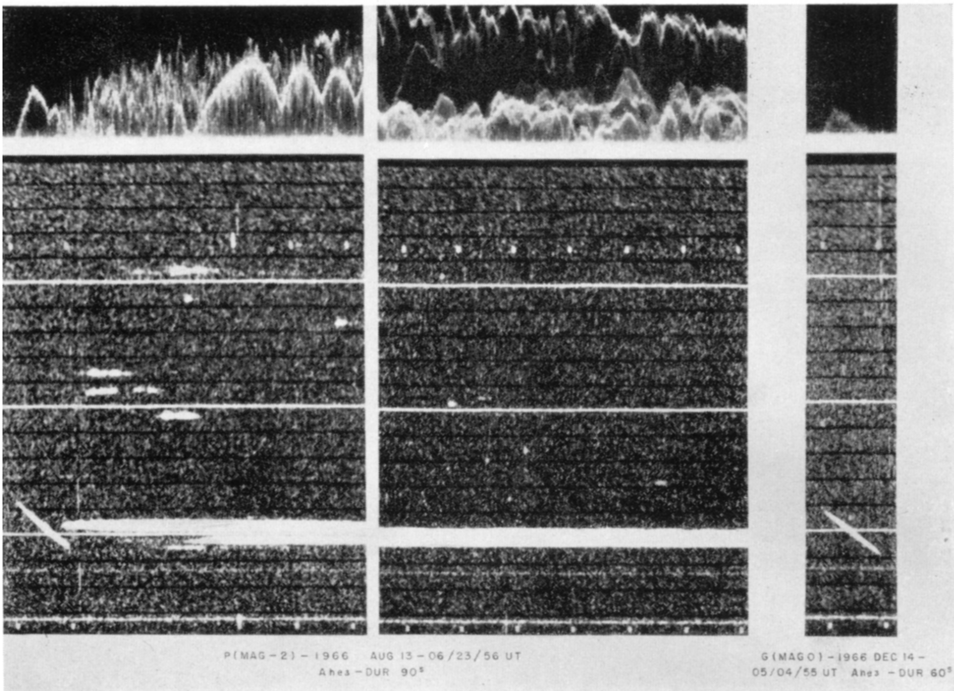

FIG. 8.

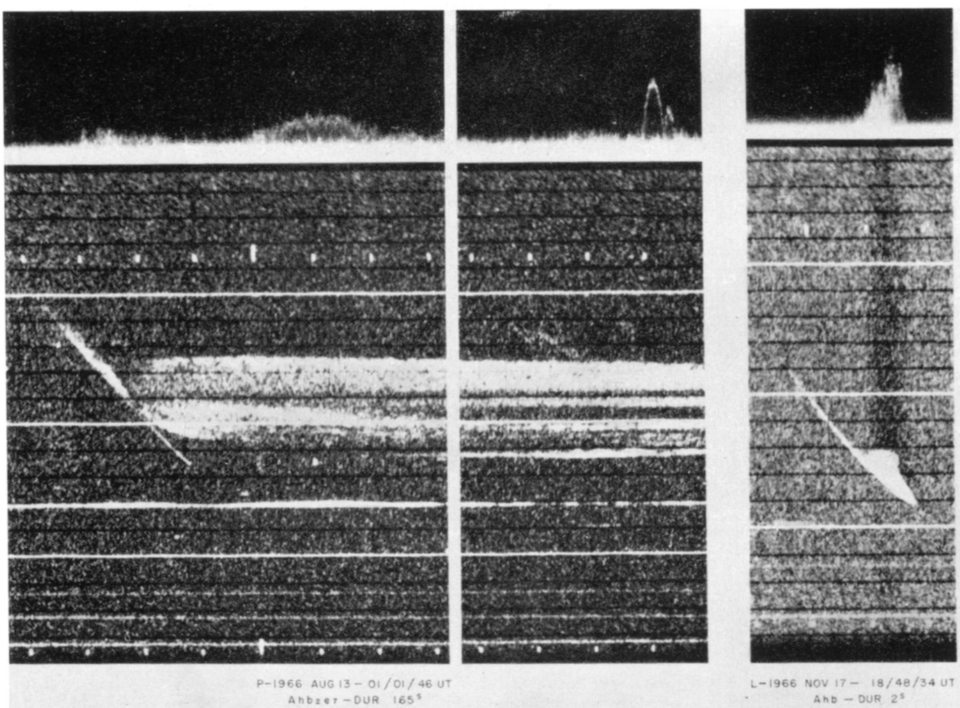

FIG. 9.

https://doi.org/10.1017/S0074180900019586 Published online by Cambridge University Press

the overdense column of electrons to diffuse to a size that will give an observable echo.

Figure 10 illustrates three more examples of *b* echoes combined with portions of *h* echoes. In general the amplitude records of *b* echoes are filled in, suggesting a multiplicity of echo sources over a large range of amplitudes. This is what might be

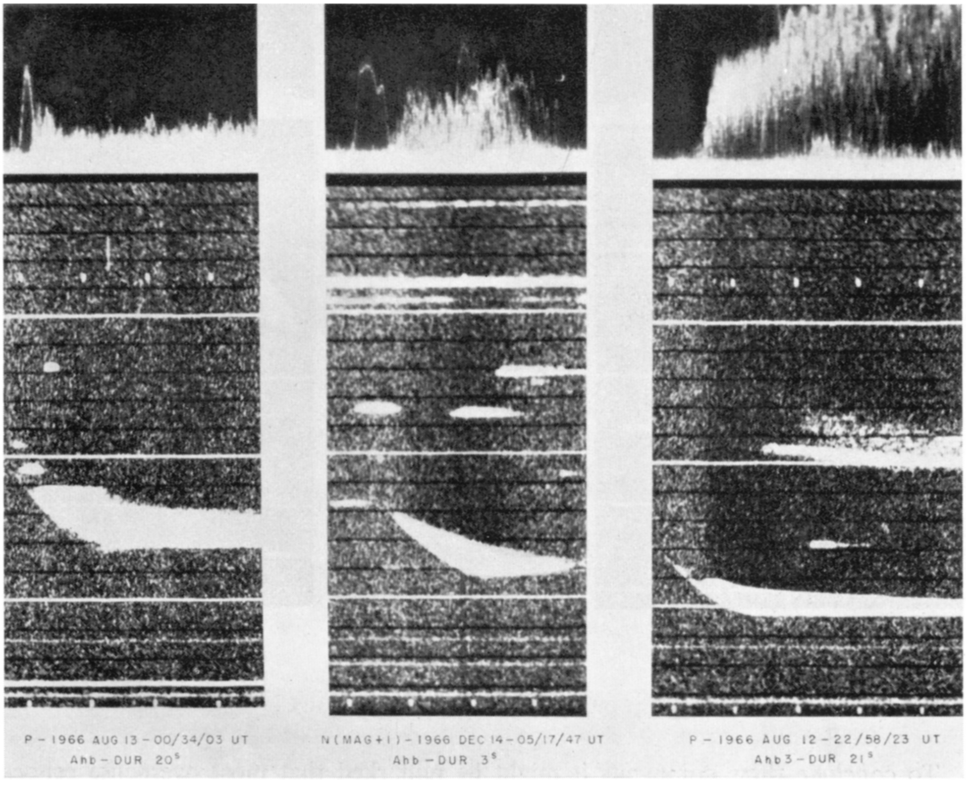

FIG. 10.

expected in the case of a relatively large, rapidly fragmenting meteoroid, the type thought to correspond to the *b* echoes (McIntosh, 1961). There is a sharp cut-off at the long-range edge of the first *b* echo shown. In the case of the third *b* echo there is some evidence of a similar cut-off and the additional echo, at 200–240 km range, probably belongs to the same meteor, which occurred when the radiant was low in the sky. It should be mentioned that on any given night the detailed echoes of very bright meteors recorded in a period of several hours often show similarities in their form. This indicates that the structure of the ionosphere at the time has its effect on the appearance of overdense echoes, a logical conclusion as upper-air winds

https://doi.org/10.1017/S0074180900019586 Published online by Cambridge University Press

obviously modify and control the form of the enduring electron column. Figure 11 gives examples of three *b* echoes for meteors that have passed the T_0 point before registering. In this case the *h* echo slopes to the right and the various *b* characteristics appear in reverse order when related to range.

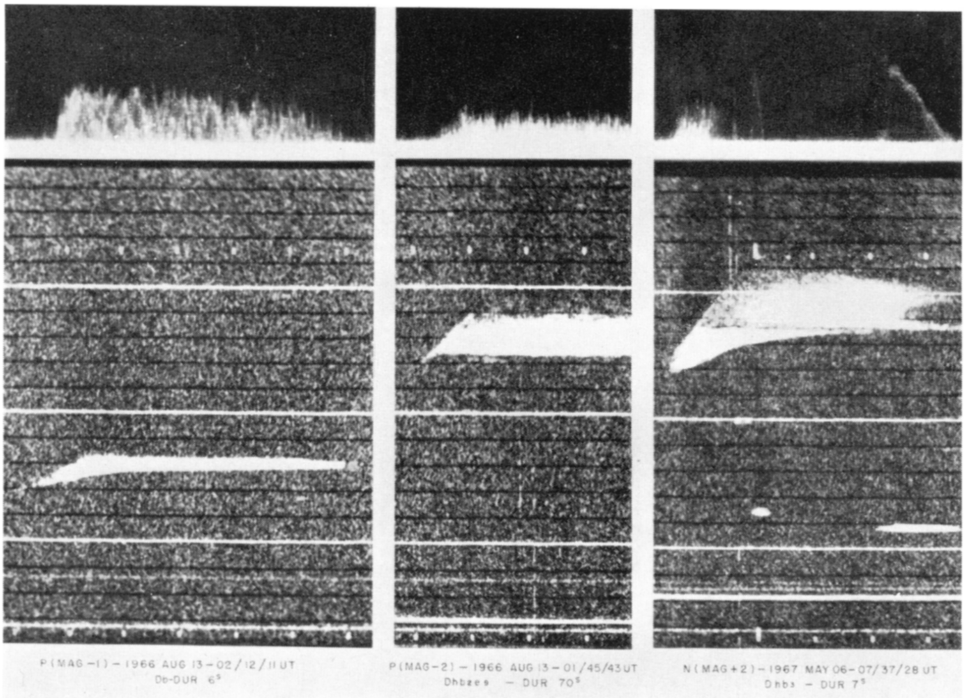

FIG. 11.

To conclude these comments it might be remarked that most overdense echoes appear much the same when viewed from widely different directions, as was shown by Millman and McKinley (1949) in the early years of the Ottawa program.

References

Appleton, E., Naismith, R. (1947) *Proc. phys. Soc. London*, **59**, 461.
Hey, J.S., Parsons, S.J., Stewart, G.S. (1947) *Mon. Not. R. astr. Soc.*, **107**, 176.
Lovell, A.C.B. (1954) *Meteor Astronomy*, Clarendon Press, Oxford.
McIntosh, B.A. (1961) *Can. J. Phys.*, **39**, 437.
McIntosh, B.A. (1962) *J. atmos. terr. Phys.*, **24**, 311.
McKinley, D.W.R. (1961) *Meteor Science and Engineering*, McGraw-Hill, New York.
McKinley, D.W.R., Millman, P.M. (1949) *Proc. Inst. Radio Eng.*, **37**, 364.
Millman, P.M. (1962) *Astr. J.*, **67**, 233.
Millman, P.M., McKinley, D.W.R. (1949) *Sky Telesc.*, **8**, 114.

https://doi.org/10.1017/S0074180900019586 Published online by Cambridge University Press

DISCUSSION

Kaiser: It is very important to realize that, when we speak of underdense and overdense trains, we are not using these words in the volume-density sense. We have a characteristic line density ($\sim 10^{14}$ m^{-1}) and, if the actual line density is less than this, the incident wave penetrates the train even if the volume density is above the critical value – in this case as an evanescent wave.

Whipple: Please expand your description of 'filling-in' of radar echoes from fragmenting meteors.

Millman: Both the range-time record and the amplitude-time record of the *b*-type echoes have an envelope with a filled-in appearence. We believe this results from the integration of a large number of electron blobs or trails produced by many individual fragments of the original meteoroid.